# COL8A2 Regulates the Fate of Corneal Endothelial Cells

Jin Sun Hwang, Dae Joong Ma, Jinju Choi, and Young Joo Shin

Department of Ophthalmology, Hallym University Medical Center, Hallym University College of Medicine, Seoul, Republic of Korea

Correspondence: Young Joo Shin, Department of Ophthalmology, Hallym University College of Medicine, Hallym University Medical Center, 1 Shingil-ro, Youngdeungpo-gu, Seoul 07441, Republic of Korea; schinn@hanmail.net.

JSH and DJM contributed equally to this work.

**Received:** April 7, 2020
**Accepted:** August 24, 2020
**Published:** September 15, 2020

Citation: Hwang JS, Ma DJ, Choi J, Shin YJ. COL8A2 regulates the fate of corneal endothelial cells. *Invest Ophthalmol Vis Sci.* 2020;61(11):26. https://doi.org/10.1167/iovs.61.11.26

**Purpose.** To investigate the effect of COL8A2 repression on corneal endothelial cells (CECs) in vitro and in vivo.

**Methods.** Cultured human CECs (hCECs) were transfected with *COL8A2* siRNA (*siCOL8A2*), and the cell viability and proliferation rate were measured. The expression of cell proliferation–associated molecules was evaluated by Western blotting and real-time reverse transcription PCR. Cell shape, Wingless-INT (WNT) signaling, and mitochondrial oxidative stress were also measured. For in vivo experiments, *siCOL8A2* was transfected into rat CECs (rCECs), and corneal opacity and corneal endothelium were evaluated.

**Results.** After transfection with *siCOL8A2*, COL8A2 expression was reduced (80%). Cell viability, cell proliferation rate, cyclin D1 expression, and the number of cells in the S-phase were reduced in *siCOL8A2*-treated cells. The cell attained a fibroblast-like shape, and SNAI1, pSMAD2, and $\beta$-catenin expression, along with mitochondrial mass and oxidative stress levels, were altered. Corneal opacity increased, and the CECs were changed in rats in the *siCOL8A2* group.

**Conclusions.** COL8A2 is required to maintain normal wound healing and CEC function.

Keywords: COL8A2, human corneal endothelial cells, wound healing process

The posterior surface of the cornea is lined by a monolayer of corneal endothelial cells (CECs) that functions as a water pump for the corneal stroma[1] via ion pumps and channels.[2] If the corneal endothelium is diseased, the cornea is not dehydrated and becomes edematous.[1] Corneal edema not only causes blindness, but also creates painful blisters in the corneal epithelium.[1] Persistent corneal edema requires corneal transplantation and can result from trauma, surgery, corneal endotheliitis, Fuchs' endothelial corneal dystrophy (FECD), or congenital hereditary endothelial dystrophy.[3] A variety of mechanisms have been studied in the context of CEC disease, including oxidative stress, endoplasmic reticulum stress, aberrant DNA methylation, inflammation, apoptosis, and autophagy. The fundamental mechanism underlying CEC disease is limited regeneration after injury. CEC diseases caused by changes in the basement membrane of CECs, such as FECD, are well known. Changes in basement membrane composition may inhibit CEC regeneration.

Type VIII collagen, a nonfibrillar collagen protein, is expressed by corneal and vascular endothelial cells.[4] It is a heterodimer composed of two distinct polypeptide chains, $\alpha$1(VIII) and $\alpha$2(VIII) (genes: *COL8A1* and *COL8A2*).[5,6] Collagen VIIIa2 (COL8A2) is the main component of Descemet's membrane (DM), the basement membrane of the corneal endothelium.[7] COL8A2 has a potential role in the maintenance of CEC integrity and structure.[8] COL8A2 is coexpressed with the activating enhancer-binding protein 2 (TFAP2, AP-2) during corneal development, and this has been reported to be associated with CEC proliferation.[9] Thus the coexpression is necessary for migration and proliferation of vascular smooth muscle cells[10] and plays an important role in hepatocellular carcinoma cell migration and invasion.[11]

Mutations in *COL8A2* are one of the causes of early-type FECD,[12] a disease in which guttae are formed in the DM, progressively causing CEC dysfunction and edema, and ultimately requiring corneal transplantation.[3] FECD associated with *COL8A2* mutations exhibits early disease manifestation, especially in younger patients.[7] *COL8A2* mutations affect DM stiffness, causing guttae to form and contributing to the onset and progression of FECD.[13] Homozygous knock-in mice with this mutation (*Col8a2(Q455K/Q455K)*) exhibited endoplasmic reticulum (ER) stress that led to hCEC death.[14] Nevertheless, the role of COL8A2 in CECs is not thoroughly understood. In this study, we investigated the role of COL8A2 in CECs by inhibiting *COL8A2* expression in vitro and in vivo.

## Methods

### In vivo Transfection of Corneal Endothelium in Rats

This study was approved by the Institutional Animal Care and Use Committee (IACUC) of Hallym University Medical Center. All procedures were performed according to the Association for Research in Vision and Ophthalmology Statement for the Use of Animals in Ophthalmic and Vision Research. Six-week-old Sprague-Dawley (SD) rats, purchased from Nara Biotech (Pyeongtaek, Korea), were used for this procedure. Five rats were included in each group. The rats were maintained in a colony room with a

12-hour light/dark cycle at 25°C for seven days before initiating experiments.

For in vivo transfection, 1 nmol of negative control siRNA (siControl) or siRNA for *COL8A2* (siCOL8A2) was injected into the anterior chamber of SD rats after paracentesis. Then, 7 mm Tweezertrodes (BTX, Holliston, MA, USA) was placed on each cornea, with the positive electrode on the siRNA-injected eye. The parameters were set at 140 V, 100 milliseconds length, 950 milliseconds interval, five pulses, and 100 V/cm$^2$. Then, a previously established corneal endothelial injury model was induced using cryoinjury two days after electroporation.[15] The cornea was cryoinjured for 10 seconds in contact with a metal rod, 3 mm in diameter, that had been frozen in liquid nitrogen for 10 minutes and then irrigated with normal saline solution (day 0). Then, the corneas were evaluated.

## Clinical Evaluation and Alizarin S Red Staining

Corneal opacity was observed by slit lamp biomicroscopy and photographed. Corneal opacity was graded with photographs at days 0, 3, 7, and 14. Corneal opacity was graded in a blinded manner as follows: grade 0 = clear cornea; grade 1 = mild corneal opacity allowing good visibility of details of the iris; grade 2 = moderate corneal opacity with partial masking of iris; and grade 3 = severe corneal opacity without a view of iris. Rats were sacrificed at day 7, or 14. Eyes were enucleated and fixed in 3.7% formaldehyde (Biosesang, Seoul, Korea). Corneal endothelial staining was performed with 0.2% alizarin red S (Sigma-Aldrich, St. Louis, MO, USA) in 0.9% NaCl (pH 4.2) for 90 seconds. The corneas were then fixed in 2.5% glutaraldehyde (Sigma-Aldrich). Then, the corneal buttons were removed, placed on cavity slides, and mounted under a coverslip (taped to the slide to flatten the cornea) with a drop of 0.9% NaCl. The endothelium was viewed under the microscopy (DM2000; Leica, Wetzlar, Germany), and photographs of the central endothelium were taken. Cells were counted at × 400 magnification.

## Cell Culture and Transfection

This study was performed in accordance with the tenets of the Declaration of Helsinki and was reviewed and approved by the institutional review board/ethics committee of Hallym University Medical Center. The cells were cultured in accordance with previously published methods.[16,17] The corneas from a total of six donors were used.[16] All the cells remained attached to the DM. The endothelial cell–DM complex was incubated for 10 minutes in 0.25% trypsin/0.02% ethylenediamine tetra-acetic acid (EDTA) solution (Invitrogen, Grand Island, NY, USA). The cells were then plated at the bottom of six-well plates coated with a fibronectin–collagen combination (FNC) coating mix (Athena Environmental Sciences, Inc., Baltimore, MD, USA). The cells were cultured in OptiMem-I media (GIBCO/BRL Life Technologies, Grand Island, NY, USA) supplemented with 8% fetal bovine serum (FBS; Cambrex Bio Science, Walkersville, MD, USA), 200 mg/L calcium chloride (Sigma Chemical Co., St. Louis, MO, USA), 0.08% chondroitin sulfate (Sigma Chemical Co.), 20 µg/mL ascorbic acid (Sigma Chemical Co.), 100 µg/mL pituitary extract (Invitrogen, Grand Island, NY), 5 ng/mL epidermal growth factor (Sigma Chemical Co., St. Louis, MO), 20 ng/mL nerve growth factor (Sigma Chemical Co., St. Louis, MO), 10 µg/mL gentamicin (Invitrogen), 100 IU/mL penicillin (Cambrex Bio Science),100 IU/mL streptomycin (Cambrex Bio Science) and 2.5 µg/mL amphotericin (Cambrex Bio Science) under 5% $CO_2$. Medium was changed every two days. Cells were cultured for 10 to 14 days until confluency and were then passaged at a ratio of 1:3 using 0.25% trypsin/0.02% EDTA solution.

To evaluate the transfection efficiency, fluorescein isothiocyanate (FITC)–conjugated siRNA (Bioneer, Daejeon, Korea) were transfected to the cells. To silence *COL8A2* expression, we used small-interference RNA (siRNA). siRNA for *COL8A2* (1296-1; sense, 5′-GUC AAG GGC ACC AAC GUG U-3′ and antisense, 5′-ACA CGU UGG UGC CCU UGA-3′) and nonspecific control siRNA (SN-1001) used as a negative control, were purchased from Bioneer Cooperation. Summarily, primary HCECs at a density of $5 \times 10^4$ cells/cm$^2$ were transfected with siRNA specific for *COL8A2* at 10 nmol/L concentrations, or with negative control siRNA, using Lipofectamine RNAiMAX (Invitrogen) according to the manufacturer's instructions. The transfections were performed at 70% confluency. After incubation for 48 to 72 hours, the cells were collected for further evaluation. The cells were separated into two groups: siRNA group targeting *COL8A2* (siCOL8A2), and a control group (siControl). The effect of *COL8A2* silencing was confirmed by western blot analysis or RT-PCR 48 hours after transfection.

## Transendothelial Electrical Resistance (TEER) and Transendothelial Electrical Potential Difference (TEPD)

Endothelial barrier function was assessed by measurement of the TEER and TEPD. The surface of 1.12 cm$^2$, 0.4 µm pore sized Transwell inserts (CLS3460, Corning Incorporated/Life Sciences, Tewksbury, Massachusetts, USA) were coated with FNC coating mix. Then, 1 mL of culture media was added to the bottom well of a 12-well tissue culture plate, and 200 µL was added to the inside of the collagen-coated Transwell insert. Cells were seeded onto each collagen-coated Transwell insert at a density of approximately 100,000 cells/insert and cultured at 37°C, 5% $CO_2$ for seven days before use and transfected with siRNA. TEER and TEPD were measured using an epithelial voltohmmeter (EVOM2; World Precision Instrument, Inc., Saratoga, FL, USA). The wells were then washed twice with serum-free medium and allowed to equilibrate for one hour at 37°C, 5% $CO_2$ before measurement.[18] TEER was measured in triplicate for each well. Each group contains four wells. STX2 chopstick electrode (4 mm wide and 1 mm thick; World Precision Instrument, Inc.) was used on the transwell TEER measurement.[19] Each experiment was repeated in triplicate.

## Cell Proliferation

Cell proliferation rate was measured using a commercial bromodeoxyuridine (BrdU) proliferation assay kit (Roche Diagnostics, GmbH, Mannheim, Germany) according to the manufacturer's protocol. Cells ($5 \times 10^3$ cells/well) were placed in 96-well plates (NUNC 167008; Thermo Fisher Scientific, Denmark) and incubated for 48 hours in a humidified atmosphere containing 5% $CO_2$. Cells were then transfected and labelled with BrdU at 37°C and 5% $CO_2$ for 72 hours. After incubating the plate in the FixDenat solution for 30 minutes at room temperature, the cells were

Investigative Ophthalmology & Visual Science

incubated with anti-BrdU-POD solution for approximately 90 minutes at room temperature. Then, substrate solution was added to each well, and the plate was incubated for 20 minutes at room temperature. Thereafter, 1 mol/L $H_2SO_4$ was added to each well to stop the reaction. The optical density was measured at 450 nm using an ELISA reader (Synergy HTX, Biotek, Winooski, VT, USA). Proliferation rates were expressed as the percentage of controls after subtraction of the corresponding blanks.

### Cell Cycle Analysis

Cell cycle analysis was performed using the Muse cell analyzer (Merck Millipore, Burlington, MA, USA) with propidium iodide (PI) staining according to the manufacturer's protocol. Briefly, cells were grown in six-well plates and transfected with siRNA; then harvested by trypsinization and washed twice with phosphate-buffered saline solution (PBS). The cells were fixed with 1 mL of 70% cold ethanol at −20°C for five hours and washed twice with PBS. After centrifugation at 1500 rpm for five minutes, the samples were treated with 200 uL solution including 50 µg/mL PI (Merck Millipore) and 100 µg/mL RNase A (Biosesang, Seongnam, Korea). The percentage of cells in G0/G1, S and G2/M phases was then calculated using a Muse cell analyzer.

### Western Blotting

Radioimmunoprecipitation assay buffer (Biosesang, Seoul, Korea), containing a p8340 protease inhibitor cocktail (one tablet/10 mL; Sigma-Aldrich) and PhosSTOP phosphatase inhibitor cocktail (one tablet/10 mL; Roche, Basel, Switzerland), was used to isolate total cellular proteins. Western blotting was conducted using standard protocols. Either 5% skim milk or gelatin was used for blocking the nonspecific binding for one hour. Primary antibodies were mouse antihuman COL8A2 antibody (sc-293350, Santa Cruz biotechnology, 1:200 dilution), rabbit antihuman cyclin D1 antibody (sc-718, Santa Cruz, 1:1000 dilution), mouse antihuman SNAI1 antibody (sc-271977, Santa Cruz, 1: 1000 dilution), rabbit antihuman pSMAD2 antibody (LF-PA20460, Abfrontier, Seoul, 1:1000 dilution), mouse antihuman SMAD2/3 antibody (sc-133098, Santa Cruz, 1:1000 dilution), rabbit antihuman GSK3$\beta$ antibody (ab32391, Abcam, 1:1000 dilution), rabbit antihuman $\beta$-catenin antibody (ab325572, Abcam, 1:1000 dilution), goat antiSLC4A11 antibody (NBP1-46156, Novusbio, 1:1000 dilution), mouse anti-notch1 antibody (sc-376403, Santa Cruz, 1:500 dilution), or rabbit anti-GAPDH antibody (LF-PA0212, Abfrontier, 1:5000 dilution). A horseradish peroxidase (HRP) conjugated secondary antibody and a WEST-Queen Western Blot Detection Kit (iNtRON biotechnology, Seongnam, Kyounggi-do, Korea) were used to detect immunoreactive bands. Data were quantified by video image analysis. Protein bands were measured by densitometry (Image J, National Institutes of Health, Bethesda, MD, USA).

### Real-Time Reverse Transcription PCR

RNA was extracted from the cultured HCECs separately using the ReliaPrep RNA Miniprep Systems (Promega Cooperation, Madison, WI, USA) according to the manufacturer's instructions. RNA concentrations were determined by ultraviolet spectrophotometry. The first-strand complementary DNA was synthesized from 0.2 µg of total RNA with oligonucleotide primers using a commercially available kit (GoScript Reverse Transcription System; Promega Cooperation). Complementary DNA samples were aliquoted and stored at –20°C until use. Real-time quantitative RT-PCR (RT-qPCR) were performed in 20-µL volumes using the AccuPower 2X GreenStar qPCR Master Mix (Bioneer) with real-time qPCR Primer Assay for human, and the following thermocycling parameters −95°C for 10 minutes then 40 cycles at 95°C for 15 seconds and at 60°C for 60 seconds. SYBR green fluorescence was measured at the end of each cycle. The $\beta$-actin gene, a housekeeping gene, was used as a standard for normalization. Primer sequences, purchased from Bioneer, were described in the Table. Assays were performed in triplicate. Melting curve analysis was performed to ensure good-quality specific PCR products. RT-qPCR results were analyzed, using the relative standard curve method and compared and calibrated against the control group.

### Mitochondrial Oxidative Stress Evaluation

MitoSOX Red (Invitrogen) was used to measure mitochondrial superoxide production according to the manufacturer's protocol. Cells ($1 \times 10^5$) were cultured in six-well plates and transfected with siRNA for 48 hours. Cells were incubated with 5 µmol/L MitoSOX reagent for 30 minutes at 37°C in the dark and then washed with PBS. Cells were harvested by trypsinization and washed twice with PBS. Fluorescence intensity in each well was measured using Muse cell analyzer at an excitation wavelength of 510 nm and an emission wavelength of 590 nm. The mean intensities of MitoSOX Red fluorescence of the three samples in each group were obtained and compared.

### MitoTracker Red Staining

MitoTracker red FM fluorescent probe (Invitrogen) was used to measure mitochondrial mass according to manufacturer's protocol. Cells ($1 \times 10^5$) were cultured in six-well plates and transfected with siRNA for 48 hours. Cells were incubated with MitoTracker red FM fluorescent probe at a final concentration of 200 nmol/L for 30 minutes and then washed with PBS. Cells were harvested by trypsinization and washed twice with PBS. Muse cell analyzer was used to measure MitoTracker red fluorescence intensity at an excitation wavelength of 532 nm and emission wavelength of 576 nm. The mean intensities of fluorescence of the three samples in each group were obtained and compared.

### Immunofluorescence Staining

Immunofluorescence staining was carried out. Briefly, hCECs cultured on coverslips for three days were transfected with a siRNA. At 48 hours after transfection, cells were fixed in 3.7% formaldehyde and permeabilized with 0.5% Triton X-100. Cells were washed with PBS and incubated with blocking solution (normal goat serum, Invitrogen) for 30 minutes. Cells were incubated with rabbit anti-zonula occludens-1 (ZO-1) antibody (sc-10804, diluted 1:100) at 4°C overnight. Cells were washed with PBS and incubated with fluorescein isothiocyanate-conjugated secondary goat anti-rabbit IgG (diluted 1:100; Invitrogen) antibodies for one hour at room temperature. Samples were mounted on slides with antifade mounting medium with

Investigative Ophthalmology & Visual Science

Table. Primers for Real-Time PCR

| | Forward | Reverse |
|---|---|---|
| COL8A2 | GGCAAAGGCCAGTACCTG | CCCCTCGTATTCCTGGCT |
| PCNA | GCGTGAACCTCACCAGTATGT | TCTTCGGCCCTTAGTGTAATGAT |
| CDK2 | CCAGGAGTTACTTCTATGCCTGA | TTCATCCAGGGGAGGTACAAC |
| CDKN2A | CATAGATGCCGCGGAAGGT | CTAAGTTTCCCGAGGTTTCT CAGA |
| SANI1 | CCCCAATCGGAAGCCTAA | CCTTTCCCACTGTCCTCAT |
| SMAD1 | TAC GCC CCC ACC TGC TTA C | TTT GTG TCC ATC GGC TGA GA |
| a-SMA | CCGACCGAATGCAGAAGGA | ACAGAGTATTTGCGCTCCGAA |
| Vimentin | TCTCTGAGGCTGCCAACCG | CGAAGGTGACGAGCCATTTCC |
| TGF-b1 | CACTCCCGTGGCTTCTAGTG | GTCTTGCAGGTGGAGAGTCC |
| CTNNB1 | AAAGCGGCTGTTAGTCACTGG | CGAGTCATTGCATACTGTCCAT |
| SLC4A11 | CCTCCAATCTCTGTGTACTGC | TTCTTGAAGTATCCCTGAGTGC |
| Notch1 | GACTTTACAGGTATATCCGGAGCAA | TGCAGATACACTGGACAATGTAGA |
| ZO1 | GTGTTGTGGATACCTTGT | GATGATGCCTCGTTCTAC |
| NOX4 | GACTTTACAGGTATATCCGGAGCAA | TGCAGATACACTGGACAATGTAGA |

4′,6-diamidino-2-phenylindole (DAPI; Vector Laboratories, Burlingame, CA, USA). For negative control, primary antibody was omitted. Slides were viewed under a fluorescence microscope (DM2000; Leica).

### Statistics

Data were expressed as mean ± standard deviation. Each experiment was repeated in triplicate. An independent *t*-test was used for comparison of two groups. Fold change means relative mRNA expression to control. Data were analyzed using GraphPad Prism software version 8.4 (GraphPad Software, Inc., San Diego, CA, USA).

## Results

### In vivo Suppression of COL8A2

After transfecting *siCOL8A2* into the corneal endothelium of SD rats, RT-qPCR was performed in rCECs. Expression of *siCOL8A2* mRNA was reduced in the corneal endothelium (4.73% ± 1.54%; Fig. 2A). Corneal opacity increased in the *siCOL8A2*-transfected cornea at day 3, 1 week, and 2 weeks after in vivo transfection ($P$ = 0.049, 0.008, and 0.001; Figs. 2B and 2C). Alizarin S red staining of the corneal endothelium revealed CEC elongation in the *siCOL8A2*-transfected cornea after in vivo transfection, which was similar to the change in shape of cultured hCECs after *siCOL8A2* transfection (Fig. 2D).

### In vitro Suppression of COL8A2

**Cell Culture and Transfection.** The hCECs were cultured and exhibited a mosaic pattern at P0 (Fig. 1A). Cells were transfected with FITC-conjugated siRNA to assess transfection efficiency. In transfected cells, FITC-conjugated siRNA is observed in the cytoplasm or nucleus as green fluorescence (Fig. 1B). Transfection efficiency was 81.67% ± 3.06%. The hCECs were transfected with *siCOL8A2*, which lead to a reduction of COL8A2 expression to 13.65% ± 8.23% compared with the siControl group, as determined by RT-qPCR. This result was also confirmed by Western blotting (15.8% ± 3.4%; Figs. 1C and 1D). The reduction in the expression of COL8A2 was sufficient for subsequent analysis.

**Corneal Endothelial Function.** To investigate barrier function, TEER and TEPD were measured after hCECs were cultured in the insert of a transwell chamber. TEER and TEPD reduced in the *siCOL8A2* group (141.8 ± 10.5 Ω and −2.63 ± 0.06 mV) compared to the siControl group (165.8 ± 8.8 Ω and −2.83 ± 0.05 mV; 24.00Ω and 0.192 mV decease; $P$ = 0.004 and 0.007, respectively; Figs. 1E and 1F). Tight junctions are important for the barrier function, and the distribution of ZO1, a major component of tight junctions,[18] was investigated by immunofluorescence staining. Immunofluorescence staining for ZO1 is shown in Figure 1G. ZO1 was densely localized and well-formed in the siControl group, and its formation decreased in slender hCECs transfected with *siCOL8A2*.

**Cell Proliferation.** Compared to siControl-treated cells, the cell proliferation rate (30.0% decrease; $P$ = 0.006 and 0.044; Fig. 3A) and the percentage of cells in S-phase (52.8% decrease; $P$ = 0.012; Figs. 3B and 3C) was reduced in *siCOL8A2*-treated cells. Next, molecules associated with cell cycle progression were investigated. Cyclin D1 protein expression (64.1% decrease; $P$ = 0.047; Figs. 3D and 3E), and mRNA expression of PCNA and CDK2 (64.8% and 58.2% decrease; $P$ < 0.001 and 0.002, respectively; Figs. 3F and 3G) decreased in the *siCOL8A2* group. In contrast, mRNA expression of CDKN2A, an inhibitor of proliferation,[20] was increased by 115.9% in the *siCOL8A2* group ($P$ < 0.019; Fig. 3H).

**Endothelial-Mesenchymal Transition (EMT).** EMT was investigated in cultured hCECs. Upon evaluating cell shape, hCECs transfected with *siCOL8A2* were slender, elongated, and spindle-shaped, whereas cells in the siControl group had a polygonal shape (Fig. 4A). EMT-associated molecules were next evaluated. pSMAD2 protein levels, which is an activated form of SMAD2 that is present at elevated levels during EMT, were reduced in the *siCOL8A2* group compared to that in the siControl group (84.3% decrease; $P$ < 0.001; Fig. 4B). SNAI1 mRNA expression, which has been implicated in EMT,[21] was reduced in the *siCOL8A2* group compared with that in the siControl group (80.5% decrease; $P$ = 0.008; Fig. 4B), and this was confirmed by Western blotting (28.5% decrease; $P$ = 0.034; Fig. 4C). The mRNA expression of SMAD1 was increased in the *siCOL8A2* group compared to that in the siControl group (77.3% increase; $P$ = 0.002; Fig. 4d). Next, EMT-associated cytoskeletal molecules were evaluated. The mRNA expression of $\alpha$-SMA, vimentin, and TGF-$\beta$1 was reduced in the

Investigative Ophthalmology & Visual Science

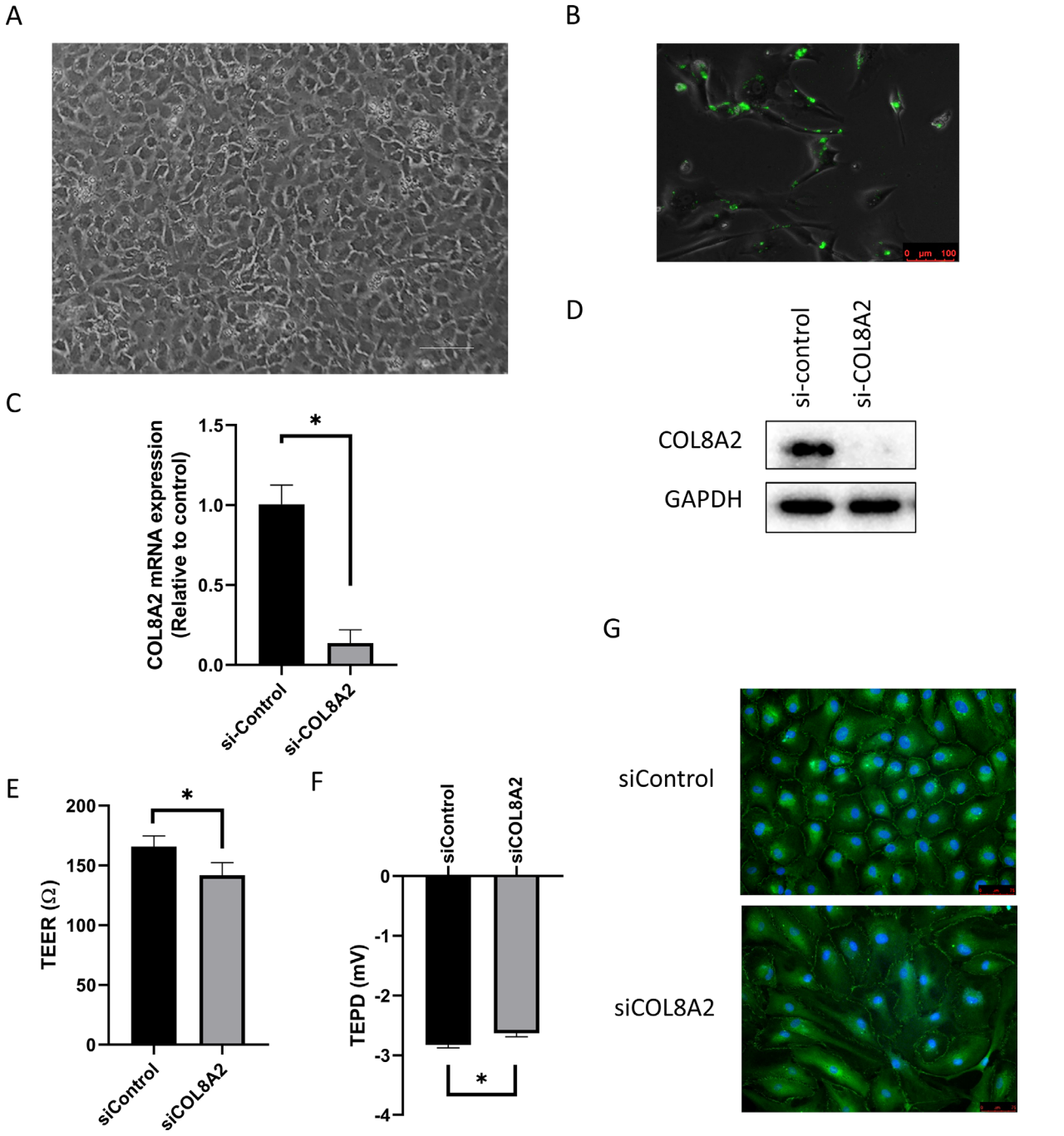


**Figure 1.** Transfection of *siCOL8A2*. (**A**) Cultured human corneal endothelial cells show mosaic pattern. Bar scale = 150 µm. (**B**) FITC-conjugated siRNA was observed after transfection. Bar scale = 100 µm. (**C** and **D**) After *siCOL8A2* transfection, COL8A2 expression was evaluated using RT-PCR, and confirmed by western blotting. (**E**) TEER and (**F**) TEPD in siControl and siCOL8A2 of cultured hCECs. TEER and TEPD were disrupted in siCOL8A2. (**G**) Immunofluorescence staining for ZO-1 (*green*). *Blue* is DAPI for nuclear staining. *Bar:* 50 µm. *Statistically significant.

*siCOL8A2* group compared to that in the siControl group (41.9%, 26.3%, and 84.3% decrease; $P = 0.007$, <0.001, and 0.006; Figs. 4E, 4F, 4G).

**Wingless-INT (WNT) Signaling.** The WNT signaling pathway was evaluated alongside EMT-related signaling. GSK3$\beta$ and $\beta$-catenin are involved in WNT signaling.[22] WNT signaling was evaluated in cultured hCECs. The expression of GSK3$\beta$ was unchanged (Fig. 5A) and mRNA expression of $\beta$-catenin was decreased in the *siCOL8A2* group compared to that in the siControl group (26.3% decrease; $P < 0.001$), which was confirmed by Western blotting (Fig. 5B). The mRNA expression of SLC4A11 was decreased in the *siCOL8A2* group compared to that in the siControl group (53.5% decrease; $P < 0.001$), which was confirmed by Western blotting (Fig. 5C). The mRNA expression of Notch1 was increased in the *siCOL8A2* group compared to that in the siControl group (307.2% increase; $P = 0.006$), which was also confirmed by Western blotting (Fig. 5D). The mRNA

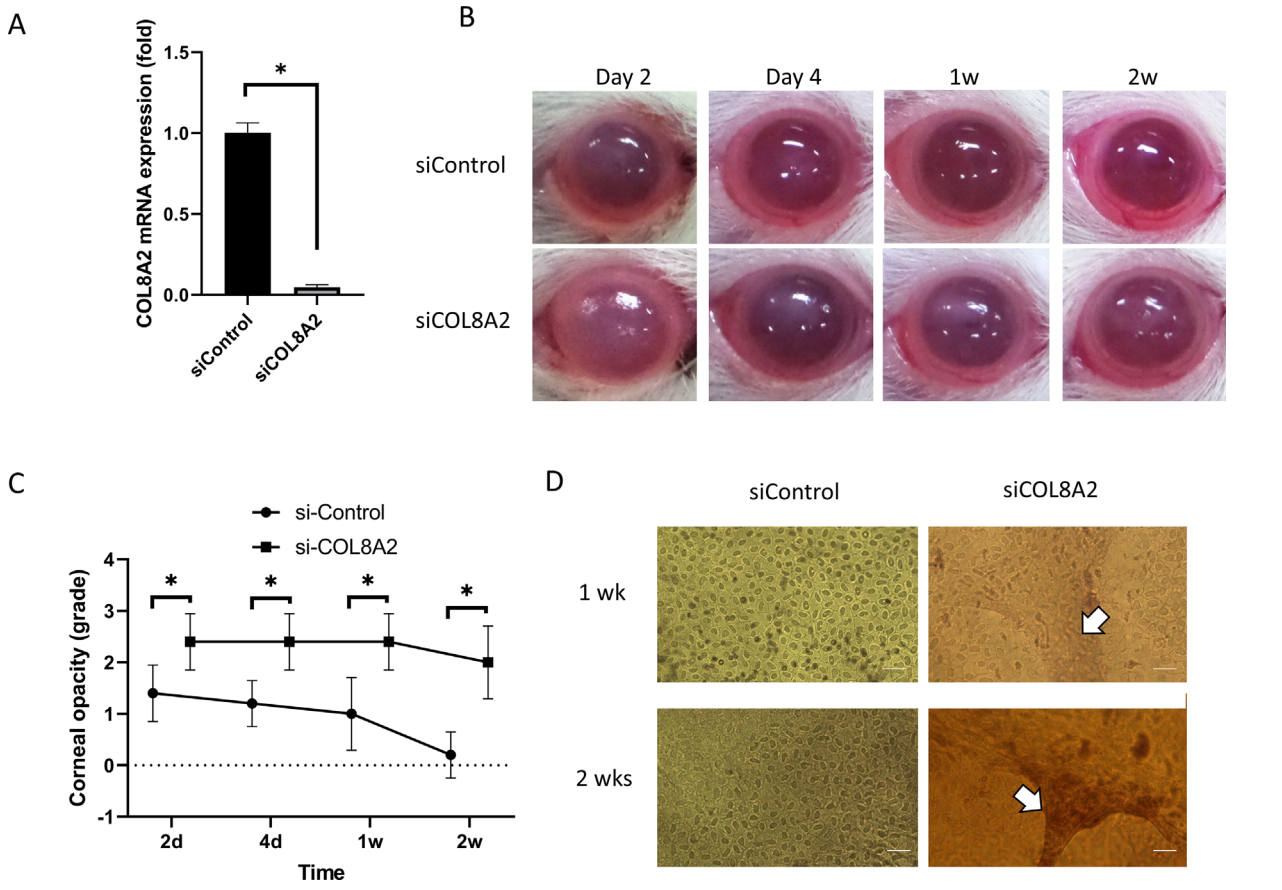


**Figure 2.** Functions of corneal endothelial cells after *siCOL8A2* transfection. (**A**) *COL8A2* mRNA expression in rat corneal endothelium after *COL8A2* siRNA transfection in vivo was reduced (4.73% ± 1.54%). Fold change means relative mRNA expression to control. (**B** and **C**) Corneal opacity during the experiments. (**D**) Alizarin S red staining showed CEC elongation, which was similar with the change in cultured cell shape after *siCOL8A2* transfection. *Bar:* 100 µm. *Statistically significant.

expression of ZO1 and NOX4 was higher in the *siCOL8A2* group compared with that in the siControl group (202.4% and 134.5% increase; $P < 0.001$ for both; Figs. 5E and 5F).

**Mitochondrial Oxidative Stress and MitoTracker Red Fluorescence Levels.** Mitochondrial oxidative stress levels were evaluated in cultured hCECs using the MitoSOX probe. Increased fluorescence intensity indicated elevated mitochondrial oxidative stress. The increase in mitochondrial oxidative stress levels (25.9% increase; $P = 0.004$; Figs. 6A and 6B) was confirmed by fluorescence imaging (Fig. 6C). The MitoTracker red fluorescence intensity decreased in the *siCOL8A2* group compared to that in the siControl group (56.6% decrease; $P < 0.001$; Figs. 6D and 6E), which was also confirmed by fluorescence imaging (Fig. 6F).

## Discussion

COL8A2 is a major component of DM, the basement membrane of hCECs, and *COL8A2* mutations have been reported to be associated with early onset of FECD. In this study, we revealed the role of COL8A2 in hCECs.

In this study, we found that corneal opacity increased in *siCOL8A2*-transfected rat corneas in vivo. In vivo, rCECs exhibited slender elongation, which was similar to the results of in vitro experiments. COL8A2 is involved in determining the structure and integrity of the cell shape.[23] Mutation of *COL8A2* led to biomechanical changes to the DM preceding endothelial cell loss in an early-onset murine model of FECD[13] and inhibition of COL8A2 impaired CEC function. Although silencing the COL8A2 gene did not disrupt the structural integrity of DM, it could change the expression of proteins present and the functions of cells.

CECs are not only a barrier between the corneal matrix and the anterior chamber but also play a role in dehydration of the stroma by pumping out ions. Thus the maintenance of TEER and TEPD is important for hCEC function. Clinically, reductions in TEER and TEPD can result in corneal edema, which can impair vision and require corneal transplantation. This study revealed that transfection with *siCOL8A2* reduced TEER and TEPD in cultured hCECs, which represents hCEC function.[18] TEER is a functional parameter for in vitro barrier systems.[19] TEER is the measurement of electrical resistance across a cellular monolayer and is a very sensitive and reliable method to assess the integrity and permeability of the monolayer.[19] TEER reflects the ionic conductance of the paracellular pathway in the epithelial or endothelial monolayer.[19] The TEER of hCECs was reported at 20 to 120 $\Omega/cm^2$,[24] which is much lower than that of corneal epithelial cells.[18] Furthermore, inhibition of COL8A2 (*siCOL8A2*) reduced TEER, indicating impaired barrier functions in hCECs. TEPD is a very sensitive index of endothelial transport generated by ionic transport.[25] It is a manifestation of the activity of endothelial fluid pumps that

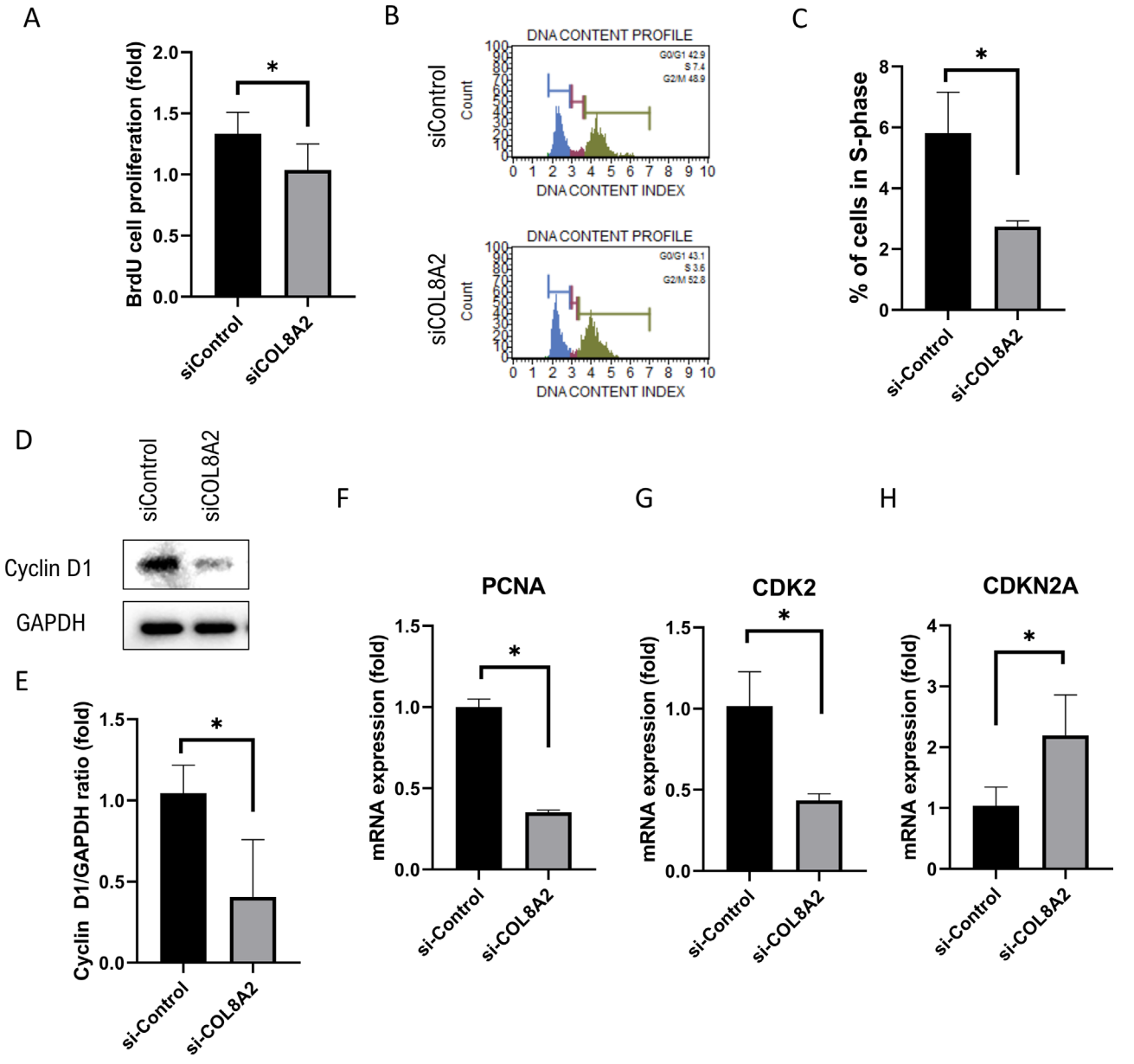


**Figure 3.** Cell proliferation. (**A**) Cell proliferation rate in siControl and siCOL8A2. (**B** and **C**) The percentage of cells in S-phase in siControl and siCOL8A2. (**D** and **E**) Cyclin D1 expression levels in siControl and siCOL8A2. (**F, G**, and **H**) mRNA expressions of PCNA, CDK2 and CDKN2A in siControl and siCOL8A2. *Statistically significant.

maintain the cornea at the level of hydration required for transparency.[4] TEPD values have been reported at 1 to 3 mV.[18] Although TEER can be applied to measure barrier function in virtually any type of cultured cell, TEER may be influenced by indeterminate regions of the cell culture outside the edges of the electrodes because it measures impedance of the culture area directly above and between the electrodes.[26] The applied boundary conditions can be identical by applying AC current between electrodes.[4] In this study, the boundary effect was not measured because the current and frequency were not changed. Therefore, there are limitations in measuring TEER.

This study demonstrated that COL8A2 plays a role in cultured hCEC proliferation. *siCOL8A2* reduced the proliferation rate, as detected by BrdU, and expression of proliferation-promoting proteins including cyclin D1 and CDK2,[27] and increased the expression of CDKN2A, a proliferation inhibitor.[20] COL8A2 has been suggested to generate a matrix environment that permits or stimulates cell proliferation,[28] and has been reported to modulate the biological effects of TGF-$\beta$1 on mesangial cells in the kidney.[29] Lack of collagen VIII in mice ameliorates mesangial cell proliferation and fibrosis.[30,31] However, our study revealed that COL8A2 inhibition in cultured hCECs suppressed EMT-related changes. COL8A2 is a key extracellular matrix protein associated with cell structure and integrity.[13] *siCOL8A2* induced changes in cell shape in vitro and in vivo, which are similarly induced during EMT or mesenchymal-endothelial transition (MET).[32] Thus, EMT-associated proteins were evaluated in cultured hCECs. SNAI1 and pSMAD2/3 expression

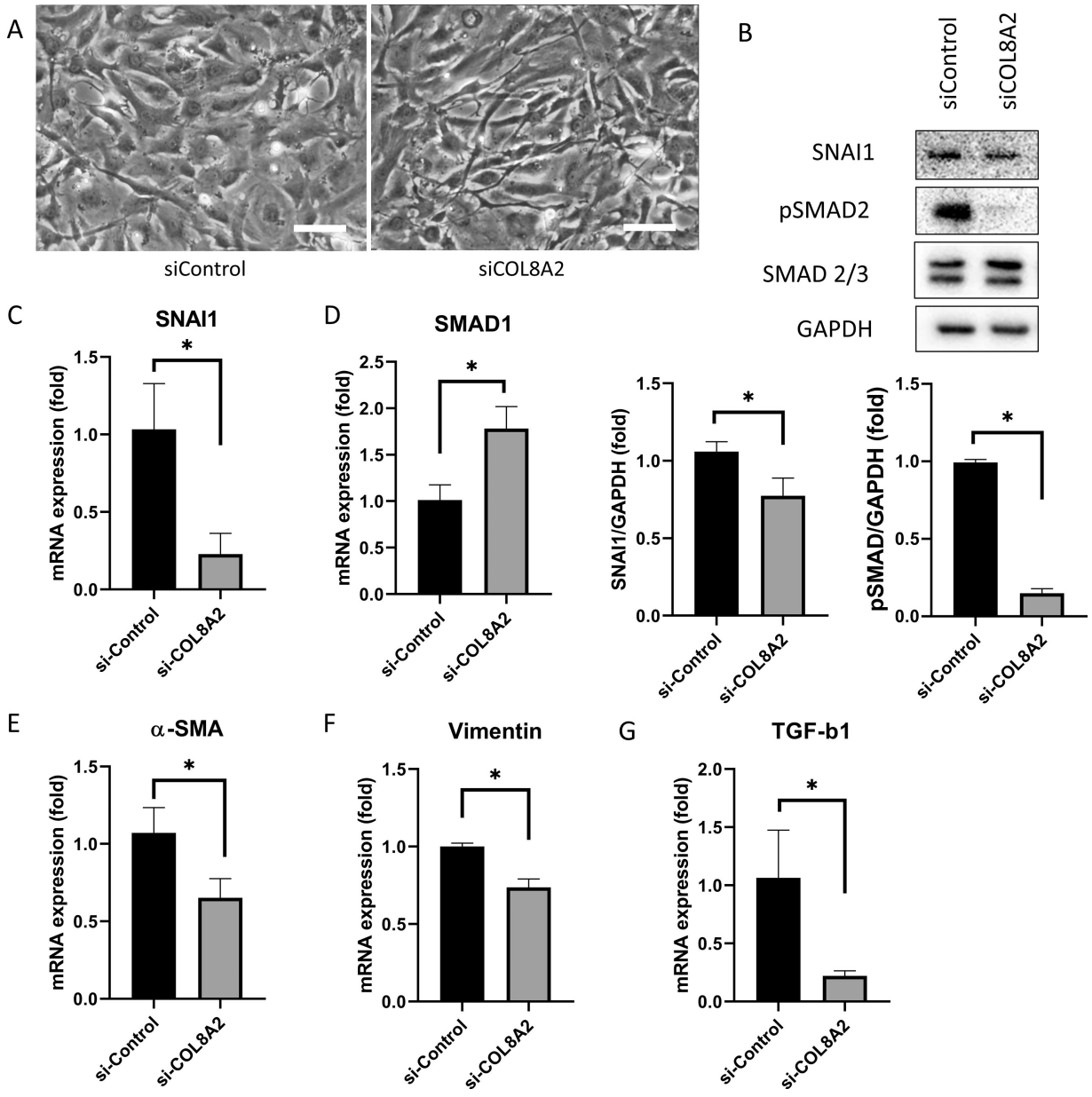


**Figure 4.** Endothelial-mesenchymal transition. (**A**) Cell shape was changed in siCOL8A2. *Bar:* 100 µm. (**B**) SNAI1 and pSMAD2 expressions in siControl and siCOL8A2. (**C**) mRNA expression of SNAI1 was reduced in siCOL8A2 compared to siControl. (**D**) mRNA expression of SMAD1 was increased in siCOL8A2 compared to siControl. (**E, F,** and **G**) mRNA expressions of $\alpha$-SMA, vimentin and TGF-$\beta$1 in siControl and siCOL8A2. *Statistically significant.

was reduced and SMAD1 expression was increased in the *siCOL8A2* group. SNAI1 interacts with SMAD signaling and controls TGF-$\beta$1-induced EMT.[33,34] The $\alpha$-SMA, vimentin, and $\beta$-catenin expression was decreased on *siCOL8A2* treatment. The $\alpha$-SMA, vimentin, and $\beta$-catenin are cytoskeletal proteins that are highly expressed during EMT.[35] The $\alpha$-SMA is an EMT marker that plays an important role in fibrogenesis.[36] Vimentin is an intermediate filament of mesenchymal origin.[22] TGF-$\beta$1 plays a role in CEC maturation and is implicated in the expression of $\alpha$-SMA and vimentin.[37] Suppression of EMT impairs cell survival, migration, and proliferation.[38] WNT signaling, an EMT-related signaling pathway,[22] was evaluated in this study. GSK3$\beta$ and $\beta$-catenin are components of WNT signaling.[22] In this study, GSK3$\beta$ expression was not changed, and $\beta$-catenin expression decreased, indicating that GSK3$\beta$ may be upstream to COL8A2 signaling. $\beta$-catenin enhances adhesion at the cell membrane and can be affected by changes in cell morphology.[39]

In this study, *siCOL8A2* altered the expression of SLC4A11, Notch1, ZO1, and NOX4, along with mitochondrial function. SCL4A11 is a $Na^+$-dependent $HCO_3^-$ co-transporter[40] and is involved in the movement of water from the stroma back to the aqueous humor.[41] SLC4A11 mutation is one of the causes of CEC diseases.[42] SCL4A11 regulates mitochondrial oxidative stress and SLC4A11 depletion impairs antioxidant signaling and increases oxidative stress in hCECs.[43] NOX4 has been reported to be associated with CEC diseases.[44] NOX4 is a member of the NADPH

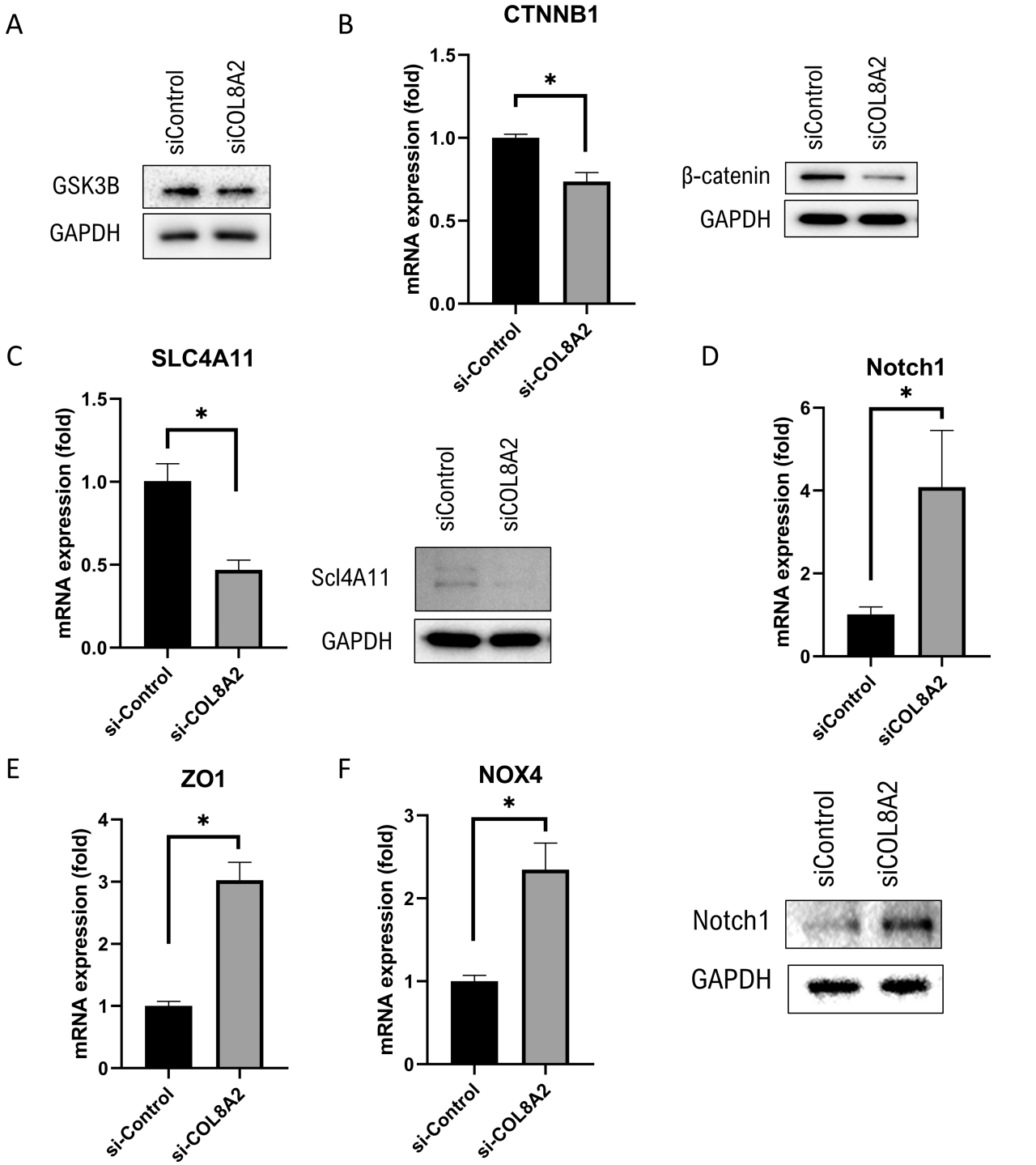


**Figure 5.** Protein and mRNA expression. (**A**) GSK3B expression was not different. mRNA expression of (**B**) $\beta$-catenin, (**C**) SLC4A11, and (**D**) Notch1 were evaluated using RT-PCR, and confirmed by western blotting. (**E** and **F**) mRNA expressions of ZO1 and NOX4 in the siControl and siCOL8A2 groups. *Statistically significant.

oxidase that regulates intracellular oxidative stress levels by producing reactive oxygen species (ROS).[37] The major source of intracellular ROS is mitochondria.[45] This study found that COL8A2 modulated mitochondrial function; mitochondrial oxidative stress increased and MitoTracker red intensity decreased, indicating mitochondrial dysfunction.[46] Oxidative stress has been reported to be a cause of CEC disease.[47] ZO1 is a tight junction protein that contributes to the barrier function of the corneal endothelium.[18] During EMT, ZO1 relocates from adhesion membrane complexes to the cytoplasm.[48] In contrast, EMT inhibition causes ZO1 to localize to the cell membrane. ZO1 expression is affected by oxidative stress.[49] Notch1 signaling regulates EMT and inhibition of Notch1 represses EMT.[50] Notch1 signaling is induced by oxidative stress and Notch1 suppresses oxidative stress-induced cell death.[51,52]

Investigative Ophthalmology & Visual Science

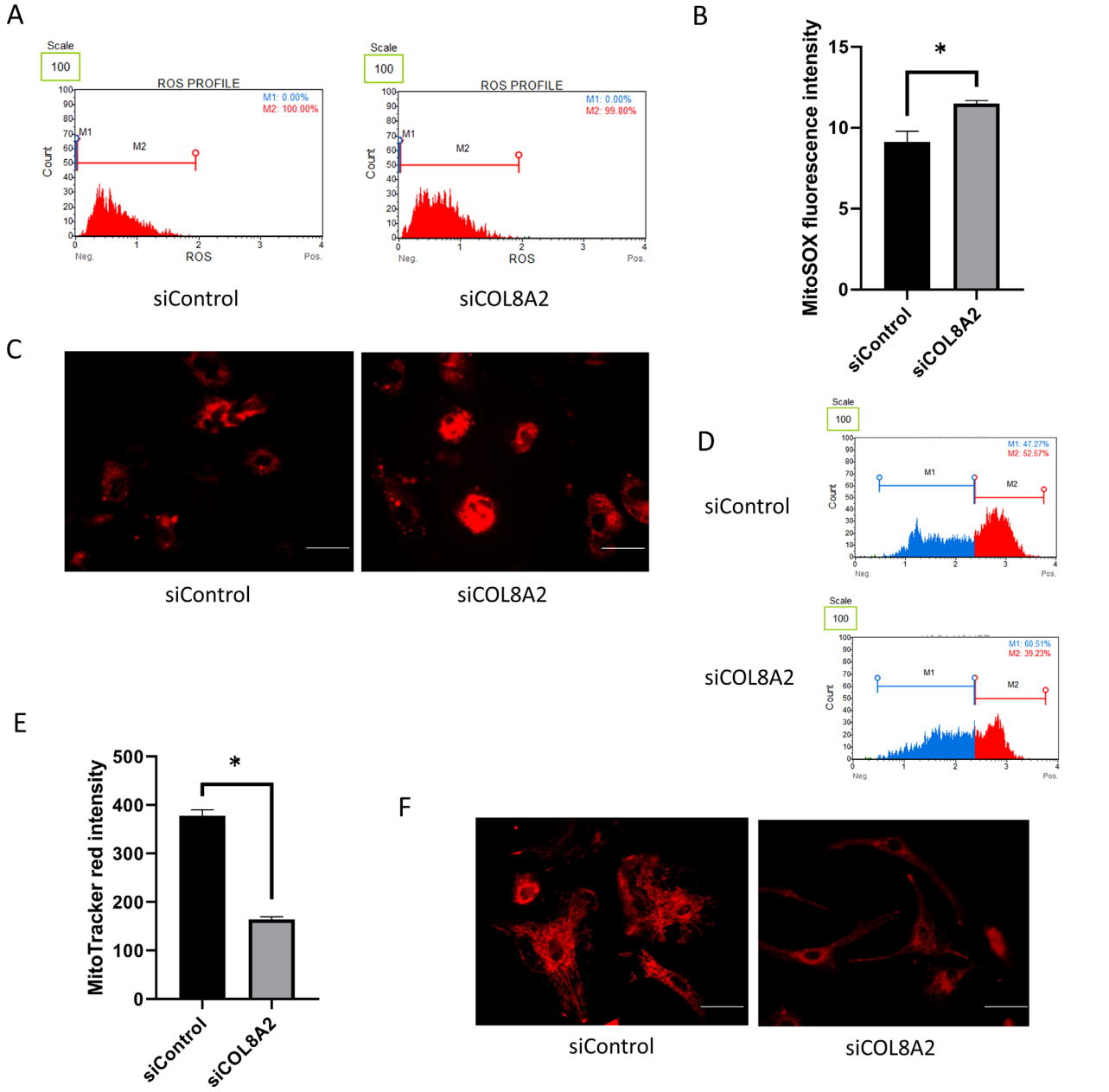


**Figure 6.** Mitochondrial functions. (**A** and **B**) Mitochondrial oxidative stress measured by MitoSOX probe in siControl and siCOL8A2. (**C**) Representative pictures for MitoSOX staining. *Bar:* 50 µm. (**D** and **E**) Mitochondria membrane potential measured by MitoTracker red. (**F**) Representative pictures for MitoTracker red staining. *Bar:* 50 µm.

Pre-existing DM in vivo may not be affected by the temporary knock-down of COL8A2, although long-term knock-down of COL8A2 distorts the structure of the DM by altering protein levels and extracellular matrix (ECM) accumulation. Temporary knock-down of COL8A2 may have more effect on cell shape and barrier function than on the structural integrity of DM. COL8A2 is not known to play a role in the ECM in normal cells. However, further study is necessary to investigate the effect on the ECM using ECM coating.

In conclusion, COL8A2 may contribute to the functions of hCECs, as well as the structural integrity of DM. COL8A2 is essential in maintaining normal CEC morphology and function, and its inhibition may play an essential role in FECD pathogenesis.

## *Acknowledgments*

Supported by the National Research Foundation (NRF) grant (NRF-2018R1A2B6002251) funded by the Korea government and Hallym University Research Fund.

Disclosure: **J.S. Hwang,** None; **D.J. Ma,** None; **J. Choi,** None; **Y.J. Shin,** None

## *References*

1. Waring GO, 3rd, Bourne WM, Edelhauser HF, Kenyon KR. The corneal endothelium. Normal and pathologic structure and function. *Ophthalmology*. 1982;89:531–590.

2. Theriault M, Gendron SP, Brunette I, Rochette PJ, Proulx S. Function-related protein expression in fuchs endothelial corneal dystrophy cells and tissue models. *Am J Pathol*. 2018;188:1703–1712.
3. Goyer B, Theriault M, Gendron SP, Brunette I, Rochette PJ, Proulx S. Extracellular matrix and integrin expression profiles in fuchs endothelial corneal dystrophy cells and tissue model. *Tissue Eng Part A*. 2018;24:607–615.
4. Akiyama R, Koniarek JP, Fischbarg J. Effect of fluorescein on the electrical potential difference across isolated rabbit corneal endothelium. *Invest Ophthalmol Vis Sci*. 1990;31:2593–2595.
5. Sage H, Trueb B, Bornstein P. Biosynthetic and structural properties of endothelial cell type VIII collagen. *J Biol Chem*. 1983;258:13391–13401.
6. Plenz GA, Deng MC, Robenek H, Volker W. Vascular collagens: spotlight on the role of type VIII collagen in atherogenesis. *Atherosclerosis*. 2003;166:1–11.
7. Gottsch JD, Sundin OH, Liu SH, et al. Inheritance of a novel COL8A2 mutation defines a distinct early-onset subtype of Fuchs corneal dystrophy. *Invest Ophthalmol Vis Sci*. 2005;46:1934–1939.
8. Liu Y, Sun H, Hu M, et al. Human corneal endothelial cells expanded in vitro are a powerful resource for tissue engineering. *Int J Med Sci*. 2017;14:128–135.
9. Hara S, Kawasaki S, Yoshihara M, et al. Transcription factor TFAP2B up-regulates human corneal endothelial cell-specific genes during corneal development and maintenance. *J Biol Chem*. 2019;294:2460–2469.
10. Marx SO, Totary-Jain H, Marks AR. Vascular smooth muscle cell proliferation in restenosis. *Circ Cardiovasc Interv*. 2011;4:104–111.
11. Wang W, Xu G, Ding CL, et al. All-trans retinoic acid protects hepatocellular carcinoma cells against serum-starvation-induced cell death by upregulating collagen 8A2. *FEBS J*. 2013;280:1308–1319.
12. Ali M, Raghunathan V, Li JY, Murphy CJ, Thomasy SM. Biomechanical relationships between the corneal endothelium and Descemet's membrane. *Exp Eye Res*. 2016;152:57–70.
13. Leonard BC, Jalilian I, Raghunathan VK, et al. Biomechanical changes to Descemet's membrane precede endothelial cell loss in an early-onset murine model of Fuchs endothelial corneal dystrophy. *Exp Eye Res*. 2019;180:18–22.
14. Jun AS, Meng H, Ramanan N, et al. An alpha 2 collagen VIII transgenic knock-in mouse model of Fuchs endothelial corneal dystrophy shows early endothelial cell unfolded protein response and apoptosis. *Hum Mol Genet*. 2012;21:384–393.
15. Chang YK, Hwang JS, Chung TY, Shin YJ. SOX2 activation using CRISPR/dCas9 promotes wound healing in corneal endothelial cells. *Stem Cells*. 2018;36:1851–1862.
16. Shin YJ, Cho DY, Chung TY, Han SB, Hyon JY, Wee WR. Rapamycin reduces reactive oxygen species in cultured human corneal endothelial cells. *Curr Eye Res*. 2011;36:1116–1122.
17. Merlini L, Angelin A, Tiepolo T, et al. Cyclosporin A corrects mitochondrial dysfunction and muscle apoptosis in patients with collagen VI myopathies. *Proc Natl Acad Sci USA*. 2008;105:5225–5229.
18. Kim E, Kim JJ, Hyon JY, et al. The effects of different culture media on human corneal endothelial cells. *Invest Ophthalmol Vis Sci*. 2014;55:5099–5108.
19. Srinivasan B, Kolli AR, Esch MB, Abaci HE, Shuler ML, Hickman JJ. TEER measurement techniques for in vitro barrier model systems. *J Lab Autom*. 2015;20:107–126.
20. Zhang S, Ramsay ES, Mock BA. Cdkn2a, the cyclin-dependent kinase inhibitor encoding p16INK4a and p19ARF, is a candidate for the plasmacytoma susceptibility locus, Pctr1. *Proc Natl Acad Sci USA*. 1998;95:2429–2434.
21. Assani G, Zhou Y. Effect of modulation of epithelial-mesenchymal transition regulators Snail1 and Snail2 on cancer cell radiosensitivity by targeting of the cell cycle, cell apoptosis and cell migration/invasion. *Oncol Lett*. 2019;17:23–30.
22. Fragiadaki M, Mason RM. Epithelial-mesenchymal transition in renal fibrosis—evidence for and against. *Int J Exp Pathol*. 2011;92:143–150.
23. Mecham RP, Ramirez F. Extracellular determinants of arterial morphogenesis, growth, and homeostasis. *Curr Top Dev Biol*. 2018;130:193–216.
24. Bartakova A, Alvarez-Delfin K, Weisman AD, et al. Novel identity and functional markers for human corneal endothelial cells. *Invest Ophthalmol Vis Sci*. 2016;57:2749–2762.
25. Koniarek JP, Lee HB, Rosskothen HD, Liebovitch LS, Fischbarg J. Use of transendothelial electrical potential difference to assess the chondroitin sulfate effect in corneal preservation media. *Invest Ophthalmol Vis Sci*. 1988;29:657–660.
26. Henry OYF, Villenave R, Cronce MJ, Leineweber WD, Benz MA, Ingber DE. Organs-on-chips with integrated electrodes for trans-epithelial electrical resistance (TEER) measurements of human epithelial barrier function. *Lab Chip*. 2017;17:2264–2271.
27. Wang J, Wang G, Ma H, Khan MF. Enhanced expression of cyclins and cyclin-dependent kinases in aniline-induced cell proliferation in rat spleen. *Toxicol Appl Pharmacol*. 2011;250:213–220.
28. Hopfer U, Fukai N, Hopfer H, et al. Targeted disruption of Col8a1 and Col8a2 genes in mice leads to anterior segment abnormalities in the eye. *FASEB J*. 2005;19:1232–1244.
29. Loeffler I, Hopfer U, Koczan D, Wolf G. Type VIII collagen modulates TGF-beta1-induced proliferation of mesangial cells. *J Am Soc Nephrol*. 2011;22:649–663.
30. Hopfer U, Hopfer H, Meyer-Schwesinger C, et al. Lack of type VIII collagen in mice ameliorates diabetic nephropathy. *Diabetes*. 2009;58:1672–1681.
31. Skrbic B, Engebretsen KV, Strand ME, et al. Lack of collagen VIII reduces fibrosis and promotes early mortality and cardiac dilatation in pressure overload in mice. *Cardiovasc Res*. 2015;106:32–42.
32. Lamouille S, Xu J, Derynck R. Molecular mechanisms of epithelial-mesenchymal transition. *Nat Rev Mol Cell Biol*. 2014;15:178–196.
33. Kaufhold S, Bonavida B. Central role of Snail1 in the regulation of EMT and resistance in cancer: a target for therapeutic intervention. *J Exp Clin Cancer Res*. 2014;33:62.
34. Xu J, Lamouille S, Derynck R. TGF-beta-induced epithelial to mesenchymal transition. *Cell Res*. 2009;19:156–172.
35. Scanlon CS, Van Tubergen EA, Inglehart RC, D'Silva NJ. Biomarkers of epithelial-mesenchymal transition in squamous cell carcinoma. *J Dent Res*. 2013;92:114–121.
36. Scharl M, Huber N, Lang S, Furst A, Jehle E, Rogler G. Hallmarks of epithelial to mesenchymal transition are detectable in Crohn's disease associated intestinal fibrosis. *Clin Transl Med*. 2015;4:1.
37. Roy O, Leclerc VB, Bourget JM, Theriault M, Proulx S. Understanding the process of corneal endothelial morphological change in vitro. *Invest Ophthalmol Vis Sci*. 2015;56:1228–1237.
38. Rodriguez-Teja M, Gronau JH, Minamidate A, et al. Survival outcome and EMT suppression mediated by a lectin domain interaction of Endo180 and CD147. *Mol Cancer Res*. 2015;13:538–547.
39. Bienz M. beta-Catenin: a pivot between cell adhesion and Wnt signalling. *Curr Biol*. 2005;15:R64–R67.


Investigative Ophthalmology & Visual Science

40. Boron WF. Sodium-coupled bicarbonate transporters. *JOP*. 2001;2:176–181.
41. Patel SP, Parker MD. SLC4A11 and the pathophysiology of congenital hereditary endothelial dystrophy. *Biomed Res Int*. 2015;2015:475392.
42. Chiu AM, Mandziuk JJ, Loganathan SK, Alka K, Casey JR. High throughput assay identifies glafenine as a corrector for the folding defect in corneal dystrophy-causing mutants of SLC4A11. *Invest Ophthalmol Vis Sci*. 2015;56:7739–7753.
43. Guha S, Chaurasia S, Ramachandran C, Roy S. SLC4A11 depletion impairs NRF2 mediated antioxidant signaling and increases reactive oxygen species in human corneal endothelial cells during oxidative stress. *Sci Rep*. 2017;7:4074.
44. Matthaei M, Zhu AY, Kallay L, Eberhart CG, Cursiefen C, Jun AS. Transcript profile of cellular senescence-related genes in Fuchs endothelial corneal dystrophy. *Exp Eye Res*. 2014;129:13–17.
45. Starkov AA. The role of mitochondria in reactive oxygen species metabolism and signaling. *Ann N Y Acad Sci*. 2008;1147:37–52.
46. Kholmukhamedov A, Schwartz JM, Lemasters JJ. Isolated mitochondria infusion mitigates ischemia-reperfusion injury of the liver in rats: mitotracker probes and mitochondrial membrane potential. *Shock*. 2013;39:543.
47. Schmedt T, Silva MM, Ziaei A, Jurkunas U. Molecular bases of corneal endothelial dystrophies. *Exp Eye Res*. 2012;95:24–34.
48. Rajasekaran AK, Hojo M, Huima T, Rodriguez-Boulan E. Catenins and zonula occludens-1 form a complex during early stages in the assembly of tight junctions. *J Cell Biol*. 1996;132:451–463.
49. Schreibelt G, Kooij G, Reijerkerk A, et al. Reactive oxygen species alter brain endothelial tight junction dynamics via RhoA, PI3 kinase, and PKB signaling. *FASEB J*. 2007;21:3666–3676.
50. Wang Z, Li Y, Kong D, Sarkar FH. The role of Notch signaling pathway in epithelial-mesenchymal transition (EMT) during development and tumor aggressiveness. *Curr Drug Targets*. 2010;11:745–751.
51. Boopathy AV, Pendergrass KD, Che PL, Yoon YS, Davis ME. Oxidative stress-induced Notch1 signaling promotes cardiogenic gene expression in mesenchymal stem cells. *Stem Cell Res Ther*. 2013;4:43.
52. Mo JS, Yoon JH, Ann EJ, et al. Notch1 modulates oxidative stress induced cell death through suppression of apoptosis signal-regulating kinase 1. *Proc Natl Acad Sci USA*. 2013;110:6865–6870.